

SUPPORTING INFORMATION

The UDP-GalNacA biosynthesis genes *gna-gne2* are required to maintain cell envelope integrity and *in vivo* fitness in multi-drug resistant *Acinetobacter baumannii*

Short title: Contribution of UDP-GalNacA to pathogenesis of *A. baumannii*

Sébastien Crépin, Elizabeth N. Ottosen, Courtney E. Chandler, Anna Sintsova,
Robert K. Ernst and Harry L.T. Mobley

CONTENTS

Fig. S1. Colonization of the bloodstream by the Δgna and $\Delta gne2$ mutants.

Fig. S2. Growth curves in LB and M9 minimal media.

Fig. S3. Resistance to normal human serum.

Fig. S4. Capsule production depends on the *gna-gne2* (*a/e2*) locus.

Fig. S5. The *gna-gne2* (*a/e2*) locus is important for twitching motility.

Fig. S6. The *gna-gne2* (*a/e2*) locus is important maintain the cell envelope integrity.

Fig. S7. Lipooligosaccharide biosynthesis is influence by the *gna-gne2* (*a/e2*) locus.

Fig. S8. Cell envelope hydrophobicity and the envelope stress response (ESR) are controlled by the *gna-gne2* (*a/e2*) locus.

Fig. S9. Resistance to antibiotics is influenced by the *gna*.

Fig. S10. Resistance to antibiotics is influenced by the *gne2*.

Table S1. *A. baumannii* strain AB0057 Gna and Gne2 closest homologs.

Table S2. Genes belonging to the KL4 locus and their associated.

Table S3. Strains and plasmids used in this study.

Table S4. Primers and oligonucleotides.

SUPPLEMENTAL FIGURE LEGENDS

Fig. S1. Colonization of the bloodstream by the Δgna and $\Delta gne2$ mutants.

Colonization of the spleen, liver and kidneys was determined by inoculating CBA/J mice via tail vein injection with 10^7 CFU of either the WT strain (57), the Δgna mutant (**A**) or the $\Delta gne2$ mutant (**B**). At 24 hpi, mice were sacrificed, organs were harvested, and the bacterial burden was determined by CFU enumeration on LB agar (57, Δgna and $\Delta gne2$) and LB-Km agar (57 eV, Δgna eV, Δgna compl., $\Delta gne2$ eV and $\Delta gne2$ compl.). Bacterial numbers are presented as the Log_{10} CFU g^{-1} of tissue. Each data point represents a sample from an individual mouse, and horizontal bars indicate the median values. Statistical significance was calculated by the Mann-Whitney test (*, $P < 0.05$; ****, $P < 0.0001$; NS, not significant). Abbreviations: 57: WT; eV: empty vector (pABBR_Km); compl.: complemented (pABBR_Km-*gna* and pABBR_Km-*gne2*).

Fig. S2. Growth curves in LB and M9 minimal media.

(A) Growth of the WT (57) and its derivative strains in LB broth. **(B)** Growth of the strains in M9 minimal medium supplemented with 0.4% glucose and 0.2% casamino acids. All results are the mean values and standard deviations of three independent experiments. For ease of reading, standard deviations were removed from graphs. The quantification of growth, or growth potential, and comparison between strains was performed by calculating the area under the curve of each

growth curve. Abbreviation: 57: WT; compl.: complemented (pABBR_Km-*gna*, pABBR_Km-*gne2* and pABBR_Km-*a/e2*).

Fig. S3. Resistance to normal human serum.

Survival in 90% normal human serum (NHS) and growth in 90% heat-inactivated human serum (HI). A total of 10^7 CFU ml⁻¹ of the WT (57) and either the Δ *gna* (A) or the Δ *gne2* (B) strains was incubated in either 90% NHS and HI, and the number of CFUs was quantified by CFU enumeration on LB agar every hour. Since no CFUs were recovered from strains Δ *gna*, Δ *gna* eV, Δ *gne2* and Δ *gne2* eV incubated with 90% NHS, no statistical tests were performed for these groups. The dashed line corresponds to the limit of detection. All results are the mean values and standard deviations of three independent experiments. Statistical significance was calculated by the Student's *t*-test (B-C, HI) (NS, not significant). Abbreviations: 57: WT; eV: empty vector (pABBR_Km); compl.: complemented (pABBR_Km-*gna* and pABBR_Km-*gne2*).

Fig. S4. Capsule production depends on the *gna-gne2* (*a/e2*) locus

(A) Microscopic analysis of capsule production. Maneval's staining of bacteria cultured for 24 h on LB agar plates. Images are representative of three independent experiments. (B) Analysis of the polysaccharides from lysates of bacteria cultured for 24 h on LB agar plates by SDS-PAGE and stained with 0.1% Alcian blue (section of the gel corresponding to the capsular polysaccharides). The strain AB5075 Δ *wzc* was used as a negative control. (C) Pellet of the strains following centrifugation of the overnight cultures normalized to an OD₆₀₀ of 1.0. The 57, AB5075 and the complemented strains present a thick and loose pellet, suggesting capsule production, while all the mutant strains show a tight and sticky pellet, which is indicative of non-capsulated strains. (D) Colony morphology of the strains cultured on BHI Congo red plates for 48 h at 37°C. (E-F) Autoaggregation assay. Cultures of WT (57) and *gna* (E) and *gne2* (F) were standardized in 10 ml of LB to an OD₆₀₀ of 2.0 in a culture tube and incubated statically at 37°C for 4 h. A 200- μ l sample was taken 1 cm below the surface at time 0 and 4 h post-inoculation for

OD₆₀₀ measurement. The percent autoaggregation was determined by dividing the OD₆₀₀ value of the aggregated cells by the OD₆₀₀ value of a control growth tube. The MDR strain AB5075 and its isogenic *wzc* mutant were used as controls (B-D). All results are the mean values and standard deviations of three independent experiments. Images are representative of three independent experiments (A-D). Statistical significance was calculated by the one-way ANOVA with Tukey's multiple comparisons test (D and E) (**, $P < 0.01$; ***, $P < 0.005$; NS, Not significant). Abbreviations: 57: WT; eV: empty vector (pABBR_Km); compl.: complemented (pABBR_Km-*gna*, pABBR_Km-*gne2* and pABBR_Km-*a/e2*).

Fig. S5. The *gna-gne2* (*a/e2*) locus is important for twitching motility

(A) Twitching motility of the bacterial strains cultured to an OD₆₀₀ 2.0 and an aliquot was stabbed to the bottom of a 1% EIKEN agar plate, then incubated at 37°C for 18 h. Twitching motility images are representative of three independent experiments. The red bars mark the twitching motility diameter. The AB5075 Δ *pilT* mutant was used as negative control. Images are representative of three independent experiments. **(B, C, D)** Quantification of the twitching diameter (in mm) from three independent experiments. The MDR strain AB5075 and its isogenic *wzc* and *pilT* mutants were used as controls (A-D). All results are the mean values and standard deviations of three independent experiments. Statistical significance was calculated by the one-way ANOVA with Tukey's multiple comparisons test (B, C, D) (*, $P < 0.05$; ***, $P < 0.005$; ****, $P < 0.001$; NS, Not significant). Abbreviations: 57: WT; eV: empty vector (pABBR_Km); compl.: complemented (pABBR_Km-*gna* and pABBR_Km-*gne2*).

Fig. S6. The *gna-gne2* (*a/e2*) locus is important maintain the cell envelope integrity

(A, B) Minimal inhibitory concentration (MIC) of vancomycin on the WT (57) and its derivative strains. MIC values were determined by E-test. **(C)** Growth of the strains on MacConkey plates. Strains were cultured to an OD₆₀₀ of 0.6 and normalized to 10⁷ CFU ml⁻¹ and serial dilutions were spotted on MacConkey plates. Images are representative of three independent experiments. **(D)** Colony morphology of the strains cultured on LB agar supplemented with BCIP-Toluidine (XP), a substrate of the periplasmic alkaline phosphatase PhoA. Images are representative of three

independent experiments. **(E, F)** Survival in the presence of polymyxin B ($1 \mu\text{g ml}^{-1}$). The number of surviving CFUs was quantified by CFU enumeration of LB agar at 15-, 30- and 60 mins p.i. The MDR strain AB5075 and its isogenic *wzc* mutant were used as controls (C,D). All results are the mean values and standard deviations of three independent experiments. Statistical significance was calculated by the one-way ANOVA with Tukey's multiple comparisons test (A) (*, $P < 0.05$; **, $P < 0.01$; ***, $P < 0.005$; NS, Not significant). Abbreviations: 57: WT; eV: empty vector (pABBR_Km); compl.: complemented (pABBR_Km-*gna* and pABBR_Km-*gne2*).

Fig. S7. Lipooligosaccharide biosynthesis is influence by the *gna-gne2 (a/e2)* locus.

Analysis of LOS extracted from of bacterial cultures cultured to mid-log phase and separated by SDS-PAGE, and stained with Pro-Q emerald 300 Lipopolysaccharide gel stain kit. The *E. coli* MG1655 (rough LPS) was used as a positive control. Images are representative of three independent experiments. Abbreviations: 57: WT; compl.: complemented (pABBR_Km-*a/e2*).

Fig. S8. Cell envelope hydrophobicity and the envelope stress response (ESR) are controlled by the *gna-gne2 (a/e2)* locus.

(A-C) Bacterial adherence to hydrocarbons. Approximately 10^7 CFU ml^{-1} were incubated with either 25% *n*-octane (A; $\Delta a/e2$ mutant) or hexadecane (B; Δgna and C; $\Delta gne2$) and the number of CFUs from the aqueous phase were recovered at 15 mins post-inoculation. An increase in the cell envelope hydrophobicity is represented by a lower number of CFUs recovered from the aqueous phase. **(D-E)** Expression of genes involved in the envelope stress response (ESR, *dsbA*, *degP*, *baeR* and *rstA*) between WT, Δgna (F), $\Delta gne2$ (G), and their respective complemented strain. Gene expression was evaluated by qRT-PCR and compared between the WT, the mutants and the complemented strain. The dashed line corresponds to the cutoff for a significant difference in expression. All results are the mean values and standard deviations of three independent experiments. Statistical significance was calculated by the one-way ANOVA with Tukey's multiple comparisons test (A-C) and by the Student's *t*-test (D,E) (*, $P < 0.05$; **, $P < 0.01$; ***, $P < 0.0001$; NS, not significant). Abbreviations: 57, WT; eV, empty vector (pABBR_Km);

compl.: complemented (pABBR_Km-*a/e2*, pABBR_Km-*gna* and pABBR_Km-*gne2*).

Fig. S9. Resistance to antibiotics is influenced by the *gna*.

(A) Minimal inhibitory concentration (MIC) of amoxicillin, gentamicin and imipenem, on WT (57) and its derivative strains. MIC values were determined by the E-test method. (B) Percent survival in the presence of a defined concentration of antibiotic. A total of 10^7 CFU ml⁻¹ were incubated in the presence of different antibiotics and the percent survival was determined by dividing the number of CFUs recovered from the antibiotic challenge by the number of CFUs recovered from the corresponding untreated sample. All results are the mean values and standard deviations of three independent experiments. Statistical significance was calculated by the one-way ANOVA with Tukey's multiple comparisons test (*, $P < 0.05$; **, $P < 0.01$; ***, $P < 0.005$; ****, $P < 0.0001$; NS, not significant). Abbreviations: 57, WT; eV: empty vector (pABBR_Km); compl.: complemented (pABBR_Km-*gna*).

Fig. S10. Resistance to antibiotics is influenced by the *gne2*.

(A) Minimal inhibitory concentration (MIC) of amoxicillin, gentamicin and imipenem, on WT (57) and its derivative strains. MIC values were determined by the E-test method. (B) Percent survival in the presence of a defined concentration of antibiotic. A total of 10^7 CFU ml⁻¹ were incubated in the presence of different antibiotics and the percent survival was determined by dividing the number of CFUs recovered from the antibiotic challenge by the number of CFUs recovered from the corresponding untreated sample. All results are the mean values and standard deviations of three independent experiments. Statistical significance was calculated by the one-way ANOVA with Tukey's multiple comparisons test (*, $P < 0.05$; **, $P < 0.01$; ***, $P < 0.005$; ****, $P < 0.0001$; NS, not significant). Abbreviations: 57, WT; eV: empty vector (pABBR_Km); compl.: complemented (pABBR_Km-*gne2*).

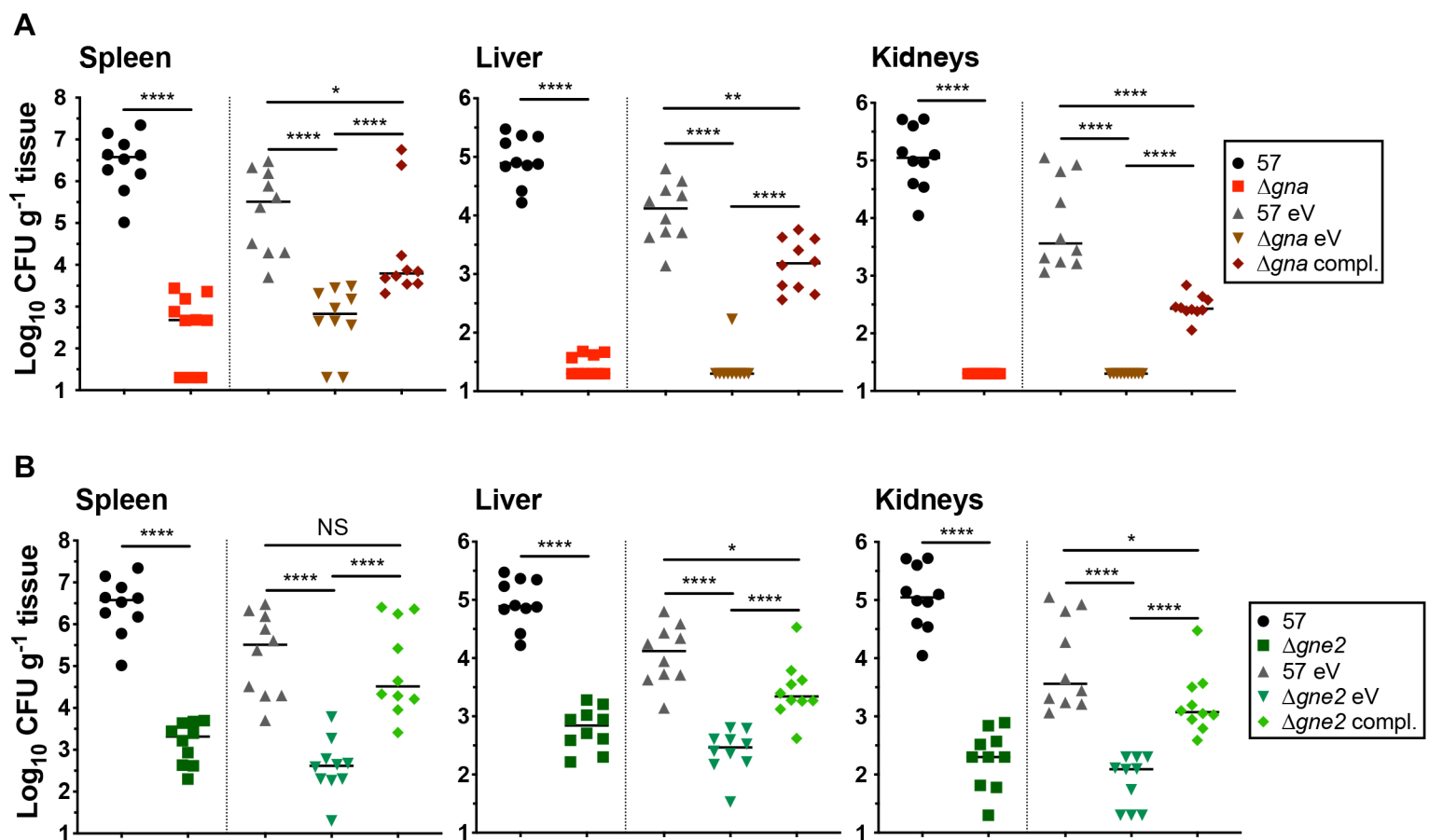
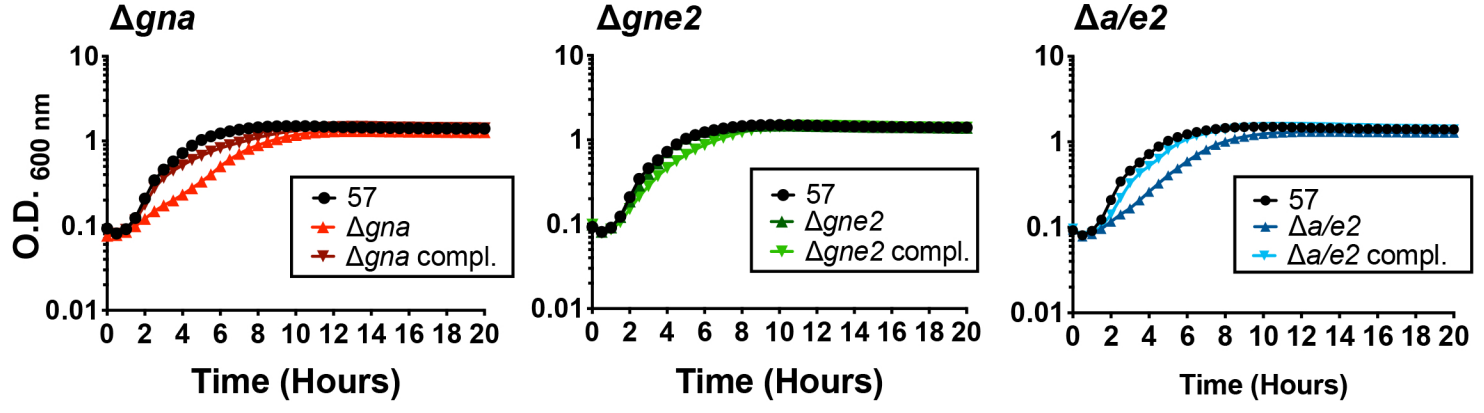


Fig. S1.

A



B

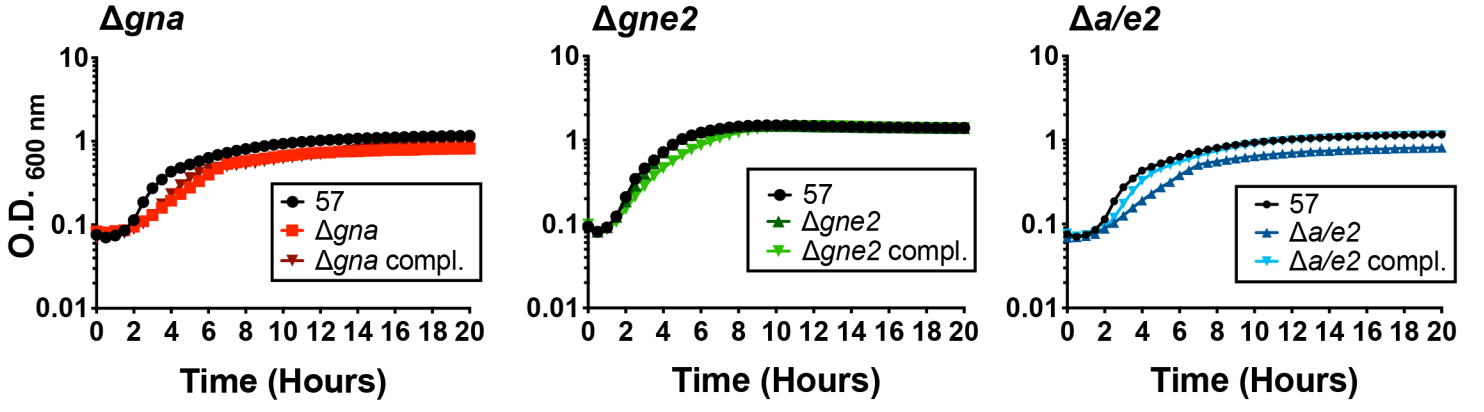
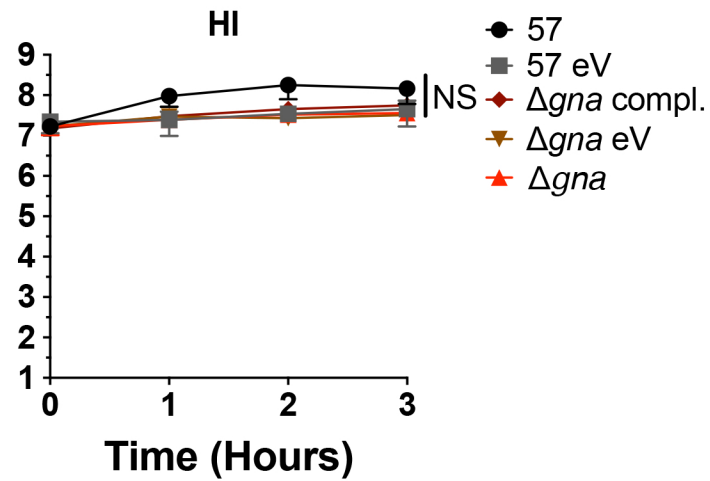
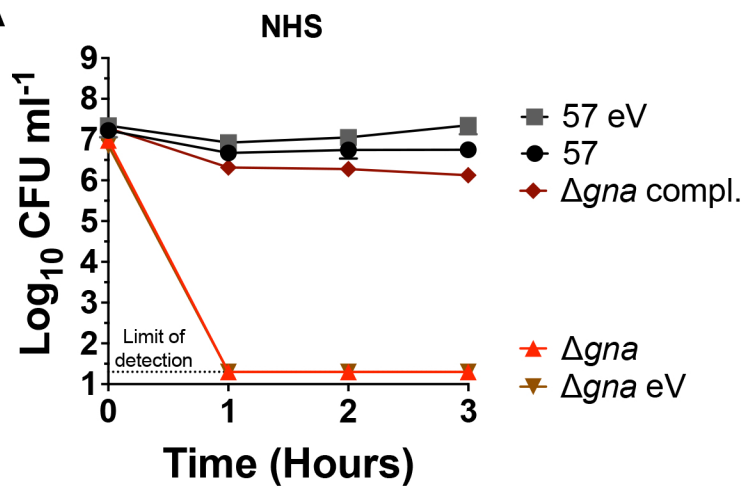
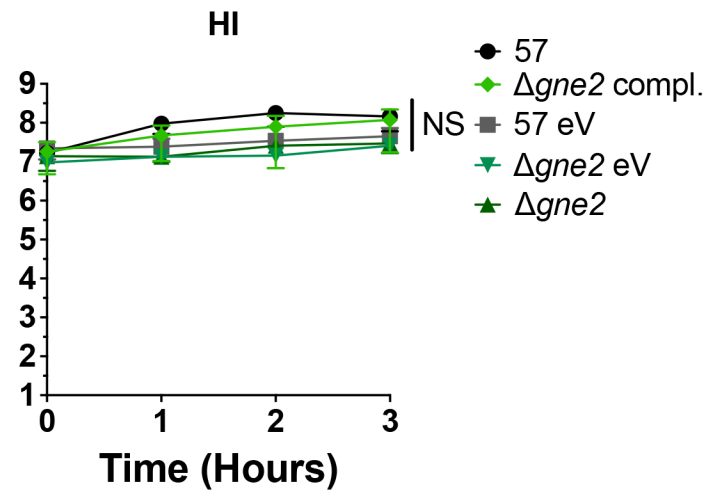
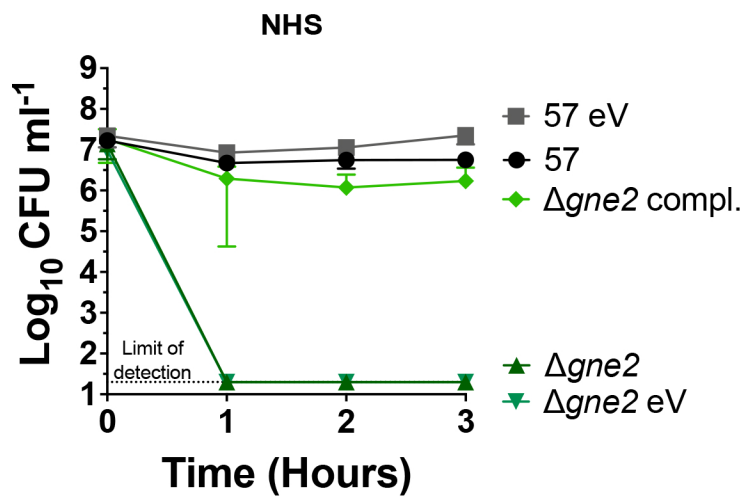


Fig. S2.

A**B****Fig. S3.**

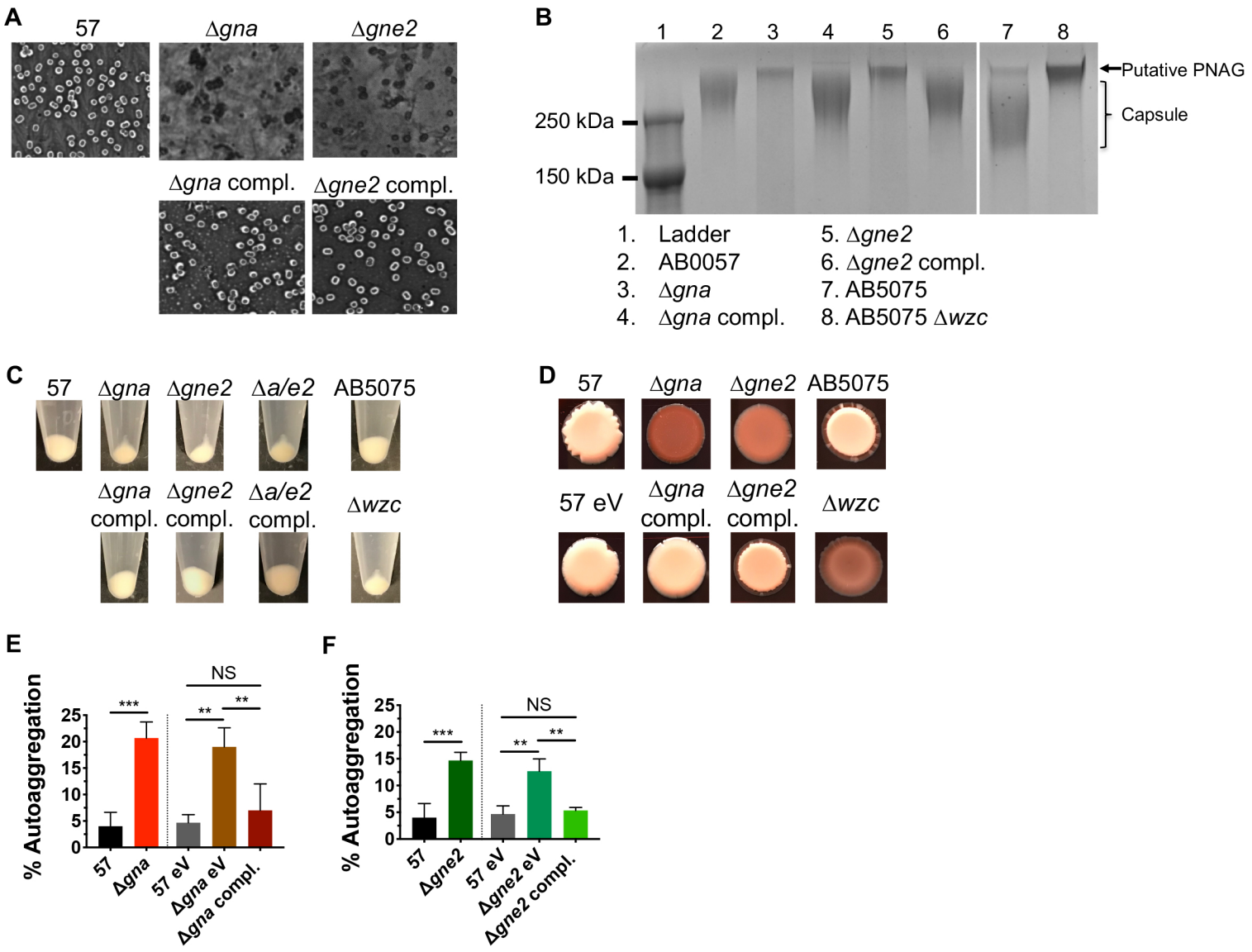


Fig. S4.

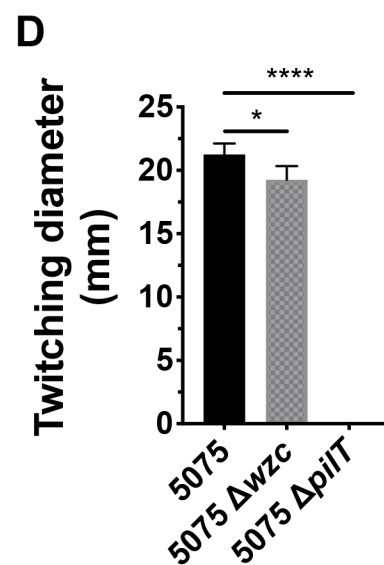
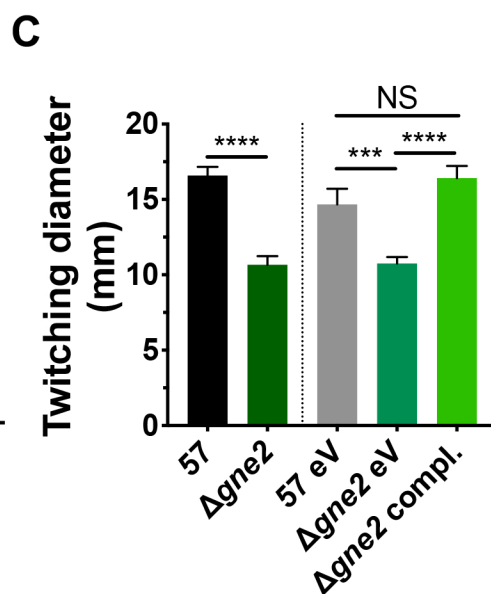
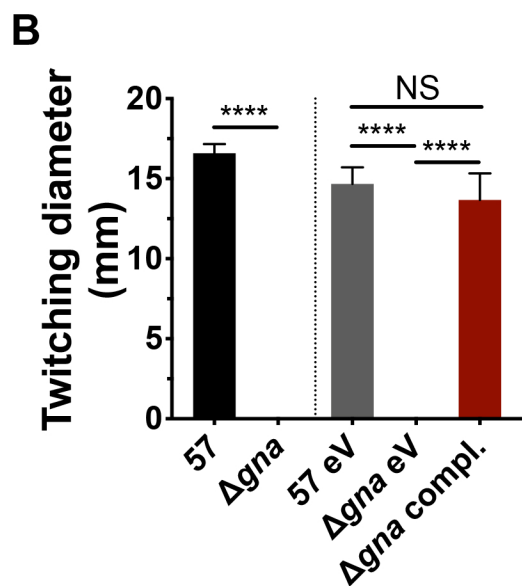
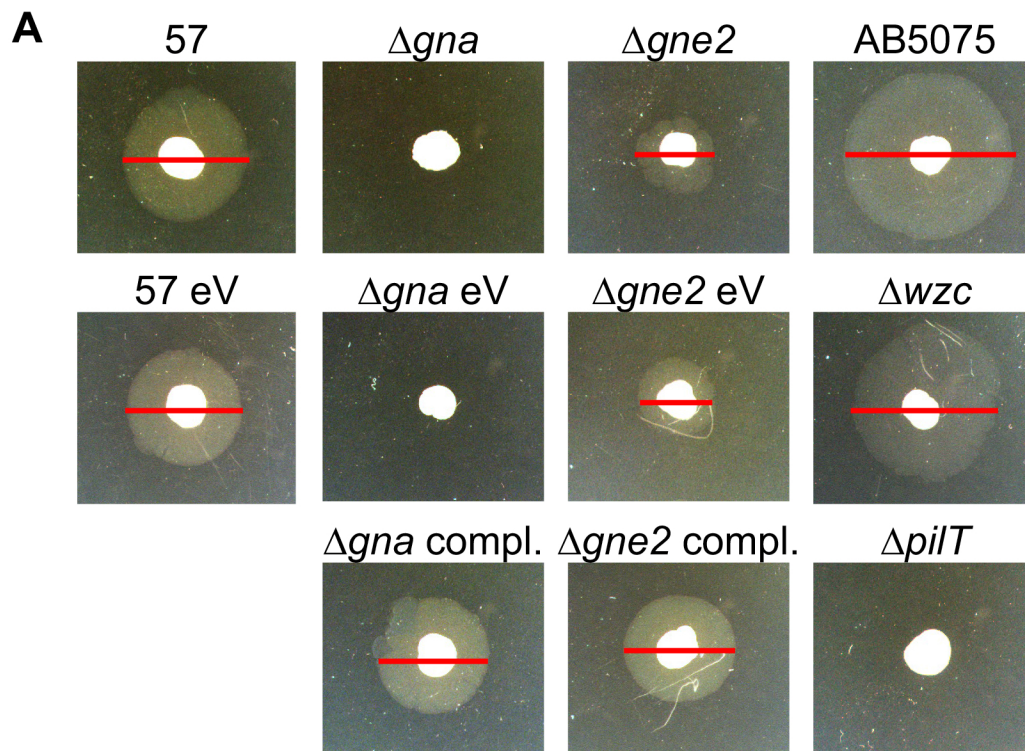


Fig. S5.

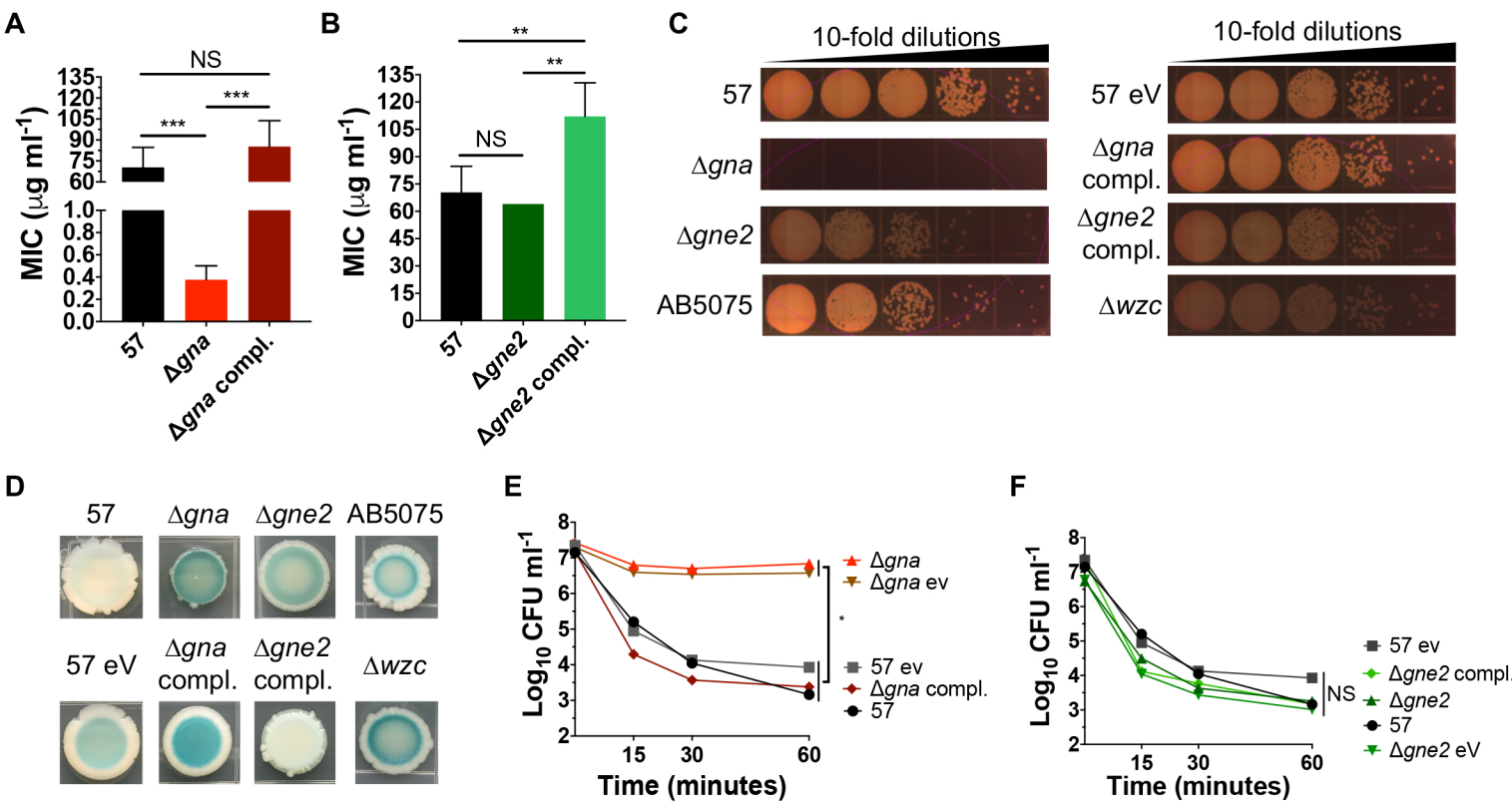


Fig. S6.

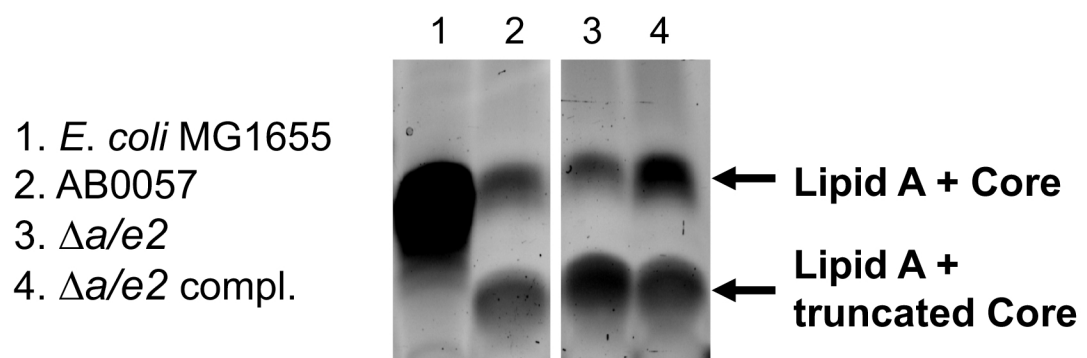


Fig. S7.

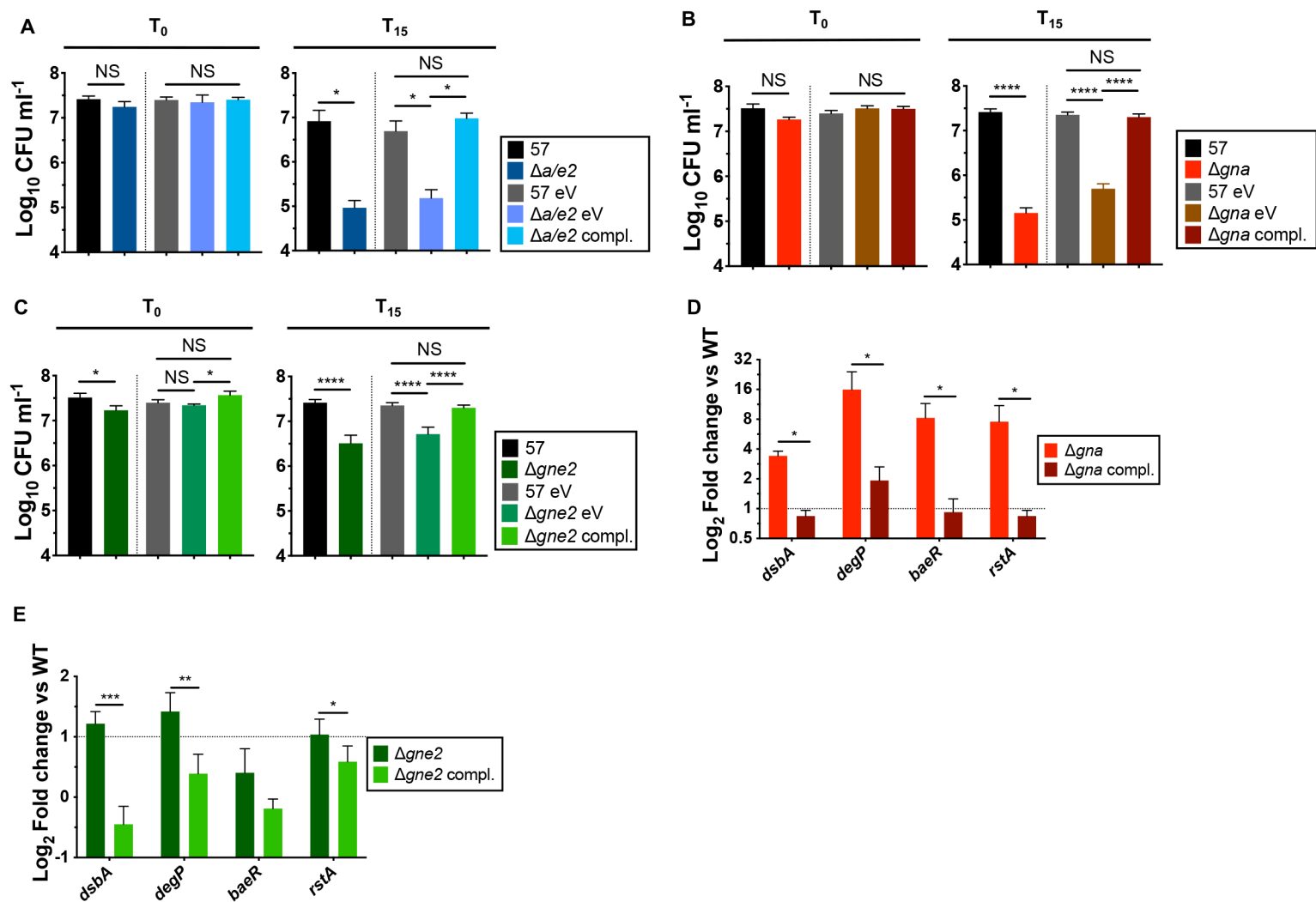


Fig. S8.

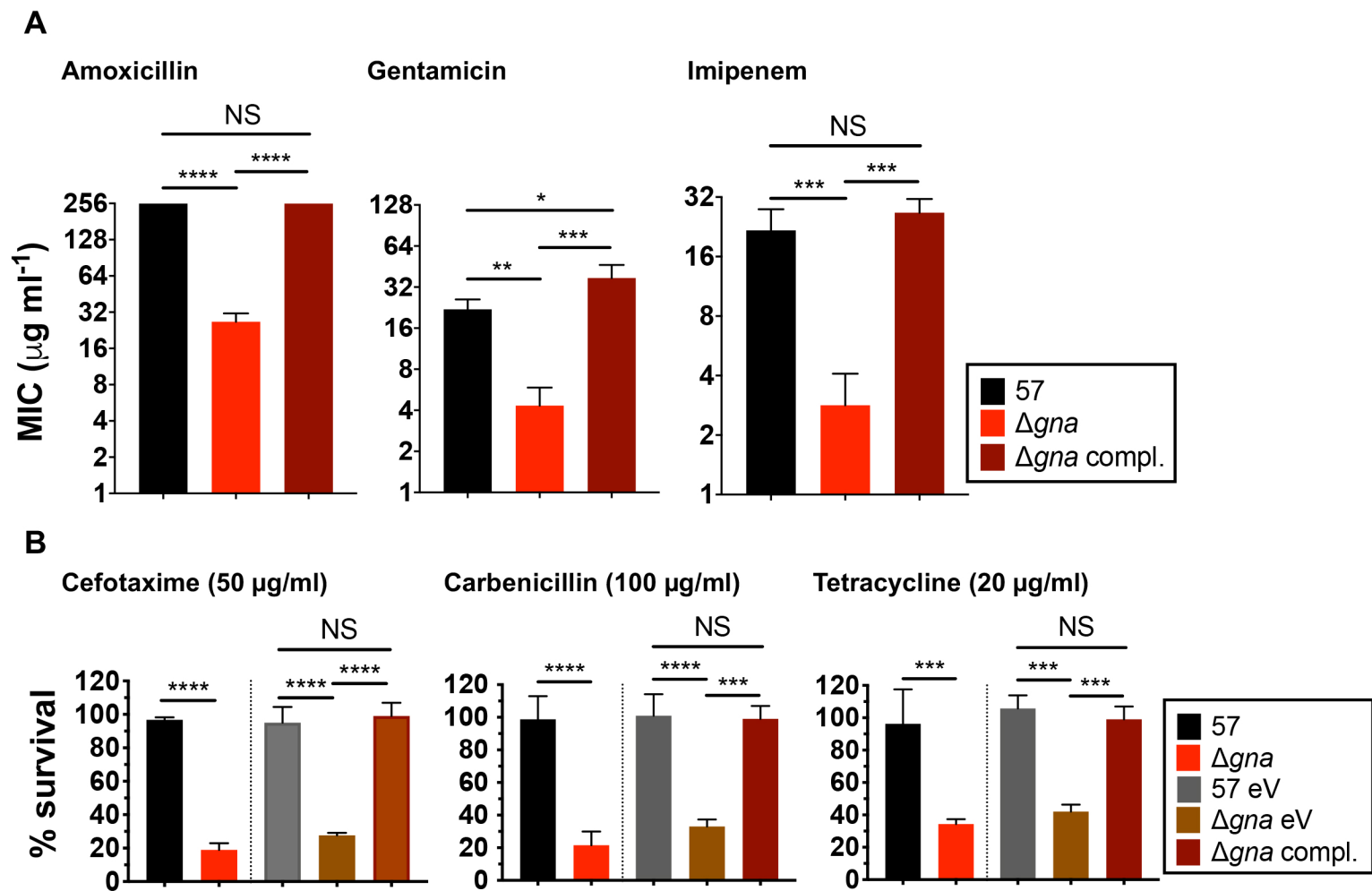
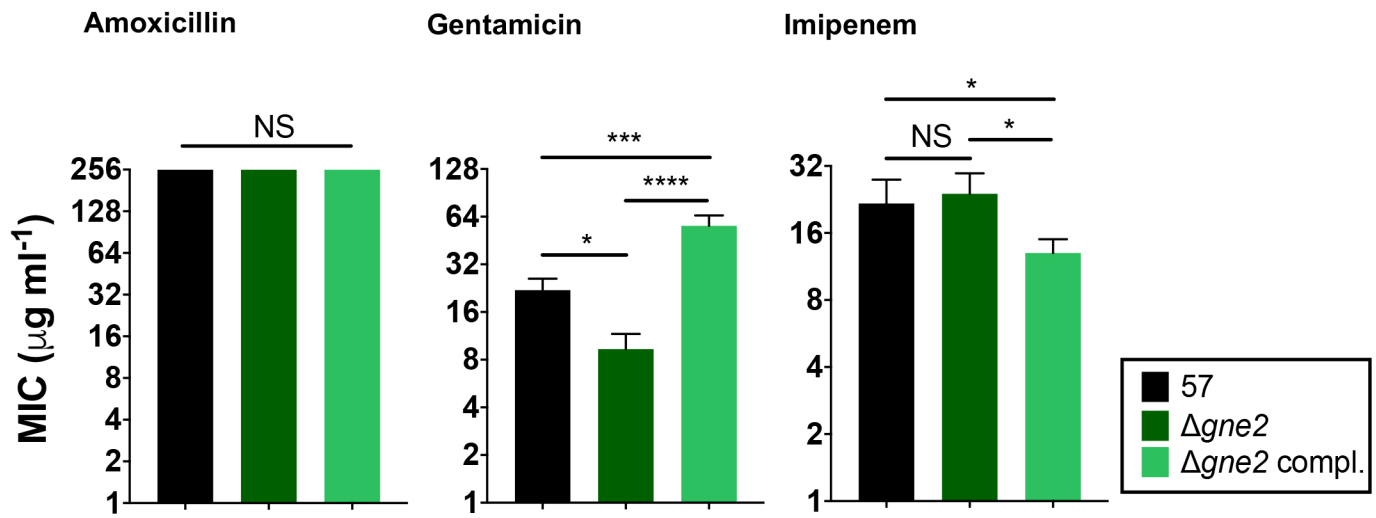


Fig. S9.

A



B

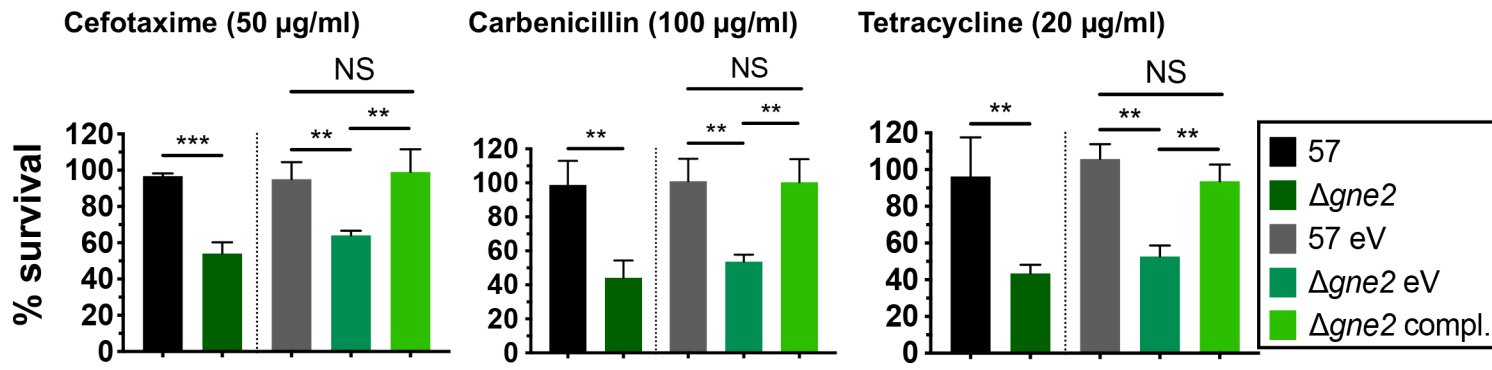


Fig. S10.

S1 Table. *A. baumannii* strain AB0057 Gna and Gne2 closest homologs.

Proteins	Predicted function	Domain	Homolog (species)	% coverage / identity / positive
Gna (TviB)	UDP- <i>N</i> -acetylglucosamine C-6 dehydrogenase	Dehydrogenase superfamily, UDP-glucose/GDP-mannose dehydrogenase family	WpbP (<i>P. aeruginosa</i>)	99 / 75 / 87
			TviB (<i>S. Typhi</i>)	99 / 69 / 84
Gne2 (TviC)	UDP- <i>N</i> -acetylglucosaminuronic acid C-4 epimerase	Epimerase superfamily, NAD dependent epimerase/dehydratase family	WpbO (<i>P. aeruginosa</i>)	98 / 73 / 86
			TviC (<i>S. Typhi</i>)	99 / 66 / 81

S2 Table. Genes belonging to the KL4 locus and their associated.

Gene	Function	Fitness defect ^a Log ₂	P value
<i>wzc</i>	Protein tyrosine kinase; involved in capsule export	-6.2	0.002
<i>wzb</i>	Low molecular weight protein tyrosine phosphatase; involved in capsule export	-8.3	0.06
<i>wza</i>	Outer membrane protein; involved in capsule export	-8.2	0.04
<i>gna</i> (<i>tviB</i>)	UDP-N-acetylglucosamine C-6 dehydrogenase	-6.9	0.053
<i>gne2</i> (<i>tviC</i>)	UDP-N-acetylglucosaminuronic acid C-4 epimerase	-8.8	0.002
<i>wzx</i>	Putative oligosaccharide-unit translocase	NA ^b	
<i>ptr1</i>	Predicted pyruvyltransferase	NA	
<i>gtr10</i>	Predicted glycosyltransferase	-1.7	0.007
<i>wzy</i>	Predicted oligosaccharide-unit polymerase	-8.2	0.1
<i>gtr11</i>	Predicted glycosyltransferase	-1.2	0.45
<i>gtr12</i>	Predicted glycosyltransferase	-7.3	0.009
<i>qnr</i>	UDP-N-acetyl-D-quinovosamine biosynthesis protein	-4.1	6.8e-5
<i>itrB1</i>	Predicted initiating transferase for oligosaccharide synthesis	-6.7	0.04
<i>atr3</i>	Predicted acetyl- or acyl- transferase	-7.3	0.005
<i>gdr</i>	UDP-N-acetyl-glucosamine 4,6-dehydratase	-5.0	3.6e-6
<i>gne3</i>	Predicted UDP-glucosamine-4-epimerase	-3.9	0.0004
<i>atr4</i>	Predicted acetyl- or acyl- transferase	-3.5	0.06
<i>atr5</i>	Predicted acetyl- or acyl- transferase	-6.9	0.004
<i>galU</i>	UTP-glucose-1-phosphate uridylyltransferase	-5.3	0.0006
<i>ugd</i>	UDP-glucose 6-dehydrogenase	-3.8	0.005
<i>gpi</i>	Glucose-6-phosphate isomerase	-5.0	7.3e-5
<i>gne1</i>	Predicted UDP-glucosamine-4-epimerase	-5.8	0.005
<i>pgm</i>	Phosphoglucomutase/phosphomannomutase	-1.6	0.0008

^a Calculated fitness defect in the spleen according to Crepin *et al.* 2018 (Crépin *et al.*, 2018)

^b Genes were not recovered from the output pools, Crepin *et al.* 2018 (Crépin *et al.*, 2018)

S3 Table. Strains and plasmids used in this study.

Strains	Characteristic(s) ^a	Source or reference
<i>E. coli</i>		
MGN-617	<i>hi thr leu tonA lacY glnV supE ΔasdA4 recA::RP4 2-Tc::Mu [pir]; Km^r</i>	(Dozois <i>et al.</i> , 2000)
MG1655	F ⁻ lambda ⁻ <i>ilvG rfb-50 rph-1</i>	(Blattner, 1997)
DH5 α λ pir	<i>sup E44, ΔlacU169 (ΦlacZΔM15), recA1, endA1, hsdR17, thi-1, gyrA96, relA1, λpir</i> phage lysogen	Laboratory collection
S17-1	<i>λpir</i> lysogen of S17.1 (Tp ^r Sm ^r <i>thi pro hsdR⁻ M⁺ recA RP4::2-Tc::Mu-km::Tn7</i>)	(Simon <i>et al.</i> , 1983)
<i>A. baumannii</i>		
57; WT; AB0057 ^{Km} ;	AB0057 <i>Δkm::FRT</i> ; Km susceptible	(Crépin <i>et al.</i> , 2018)
57 eV	AB0057 ^{Km} + pABBR_Km; Km ^R	(Crépin <i>et al.</i> , 2018)
<i>Δgna</i>	AB0057 ^{Km} <i>Δgna</i>	This study
<i>Δgna</i> eV	AB0057 ^{Km} <i>Δgna</i> + pABBR_Km; Km ^R	This study
<i>Δgna</i> compl.	AB0057 ^{Km} <i>Δgna</i> + pABBR_Km- <i>gna</i> ; Km ^R	This study
<i>Δgne2</i>	AB0057 ^{Km} <i>Δgne2</i>	This study
<i>Δgne2</i> eV	AB0057 ^{Km} <i>Δgne2</i> + pABBR_Km; Km ^R	This study
<i>Δgne2</i> compl.	AB0057 ^{Km} <i>Δgne2</i> + pABBR_Km- <i>gne2</i> ; Km ^R	This study
<i>Δgna-gne2 (Δa/e2)</i>	AB0057 ^{Km} <i>Δgna-gne2 (Δa/e2)</i>	(Crépin <i>et al.</i> , 2018)
<i>Δgna-gne2 (Δa/e2)</i> eV	AB0057 ^{Km} <i>Δgna-gne2 (Δa/e2)</i> + pABBR_Km; Km ^R	This study
<i>Δgna-gne2 (Δa/e2)</i> compl.	AB0057 ^{Km} <i>Δgna-gne2 (Δa/e2)</i> + pABBR_Km- <i>gna-gne2 (a/e2)</i> ; Km ^R	This study
AB5075	MDR Tibia/osteomyelitis isolate	(Jacobs <i>et al.</i> , 2014)
AB5075 <i>Δwzc</i>	AB5075 <i>Δwzc</i>	(Tipton <i>et al.</i> , 2018)
AB5075 <i>ΔpilT</i>	ABUW <i>Δ3031::T26 tna1_kr121205p08q137</i>	(Gallagher <i>et al.</i> , 2015)
Plasmids		
pCVD442_MCS	pCVD442 + MCS; The IS1 element was swapped by a MCS; Ap ^r , R6K, <i>sacB</i>	(Crépin <i>et al.</i> , 2018)
pCVD_Km	pCVD442_MCS_Amk; Amk ^r , R6K, <i>sacB</i>	This study

pCVD_AmK_Δ <i>gna-gne2</i> (<i>a/e2</i>)	Δ <i>gna-gne2</i> (Δ <i>a/e2</i>) in pCVD_AmK; Amk ^r , R6K, <i>sacB</i>	(Crépin <i>et al.</i> , 2018)
pCVD_Km_Δ <i>gna</i>	Δ <i>gna</i> in pCVD_Km; Kmk ^r , R6K, <i>sacB</i>	This study
pCVD_Km_Δ <i>gne2</i>	Δ <i>gne2</i> in pCVD_Km; Kmk ^r , R6K, <i>sacB</i>	This study
pABBR_Km	pABBR_MCS_Km; Km ^r	(Crépin <i>et al.</i> , 2018)
pABBR_Km- <i>gna-gne2</i> (<i>a/e2</i>)	Genes <i>gna-gne2</i> cloned into pABBR_Km; Km ^r	This study
pABBR_Km- <i>gna</i>	Gene <i>gna</i> cloned into pABBR_Km; Km ^r	This study
pABBR_Km- <i>gne2</i>	Gene <i>gne2</i> cloned into pABBR_Km; Km ^r	This study

S4 Table. Primers and oligonucleotides.

Name	Sequence 5' → 3'	Purpose
Mutant		
GA_pCVD_Km_F	GGCAGGTATATGTGATGGGTTAAAAA GGA	Inverted PCR of pCVD_Km to clone, by Gibson assembly, the gene of interest (<i>goi</i>)
GA_pCVD_Km_R	GGCAACTTTATGCCCATGCAACA	
GA_gna_5'frag_F	<u>TAGTTTCTGTTGCATGGGCATAAAGTT</u> <u>GCCGCCTAAAGCATCCGTTAAAGTCAT</u>	Amplification of ~ 1 Kb upstream of <i>gna</i>
GA_gna_5'frag_R	<u>GTCGAATATCTGACTCTGCTTGAGAA</u> <u>CCTATAATCGCTATTCTTAAATCGGCA</u> AGTTG	
GA_gna_3'frag_F	<u>CGATTTAAGAATAGCGATTATAGGTT</u> <u>CTCAAGCAGAGTCAGATATTCGACTA</u> TAAATC	Amplification of ~ 1 Kb downstream of <i>gna</i>
GA_gna_3'frag_R	<u>CCTTTTTAACCCATCACATATACCTGC</u> <u>CGCCTGTGAATGCCTTACATCTCC</u>	
delta_gna_screen	ATAAGCTTACTGTCCCAAACGGTCTA	Screening to confirm the <i>gna</i> mutation; used with GA_gna_3'frag_R
GA_gne2_5'frag_F	TCTGTTGCATGGGCATAAAGTTGCCG CCATTGGCAGTTGAGTTTGA	Amplification of ~ 1 Kb upstream of <i>gne2</i>
GA_gne2_5'frag_R	TTTTAGTACTATACCAGTTGATTGCTT GCTCACATATTGTTTGATATTGGCTCA TTTT	
GA_gne2_3'frag_F	CCAATATCAAACAATATGTGAGCAAGC AATCAACTGGTATAGTACTAAAATTTA GTCTTTG	Amplification of ~ 1 Kb upstream of <i>gne2</i>
GA_gne2_3'frag_R	CCTTTTTAACCCATCACATATACCTGC CGCCTGTGAATGCCTTACATCTCC	
delta_gne2_screen	TTTACTGGAGGCGTAATTTTCAGGGTAT G	Screening to confirm the <i>gne2</i> mutation; used with GA_gne2_3'frag_R
pCVD_Screen_F	GATTTGCAGACTACGGGCCTAAAG	Screening to confirm the cloning of the Δ <i>goi</i> into pCVD_Km
pCVD_Screen_R	CGAACTAAACCCTCATGGCTAACG	
Complementation		
AB0057_gna-gne2_F_Nrul	ACAAGTTCGCGATAAACGCAGGCTGA ACAGATTCTAGC	Cloning of the <i>gna-gne2</i> locus into pABBR_Km
AB0057_gna-gne2_R_Sall	AAATCGTGCAGCACAACCCCACTCTAT TGAGAGGTATTTTCA	

GA_pABBR_Km_R	GCCTTCCCCATTATGATTCTTCTCG	Inverted PCR of pABBR_Km to clone, by Gibson assembly, the <i>goi</i>
GA_pABBR_Km_F	ACGATTCCGAAGCCCAACCTTT	
GA_AB0057_gna_F_pABBR	<u>CGAGAAGAATCATAATGGGAAGGC</u> TAAACGCAGGCTGAACAGATTCTAG	Cloning, by Gibson assembly, of <i>gna</i> , with its native promoter, into pABBR_Km
GA_AB0057_gna_R_pABBR	<u>ATGAAAGGTTGGGCTTCGGAATCGTG</u> ATCAGCAATGGAACGAGGTACT	
GA_AB0057_gne2prom_F_pABBR	<u>TCATAATGGGAAGGCC</u> CCCTTTGTGT ATTTATCTTTAATTTGATATTGTCCAC	Cloning, by Gibson assembly, of <i>gne2</i> , with the native promoter found upstream of <i>gna</i> , into pABBR_Km
GA_AB0057_gne2prom_R_gne2	<u>TTTGATATTGGCTCAT</u> AAAAGTTAGCC TTGTTCTTACAAATTGTAT	
GA_AB0057_gne2_F_gne2prom	<u>AACAAGGCTAACTTTT</u> ATGAGCCAATA TCAAACAATATGTGAGCA	
GA_AB0057_gne2_R_pABBR	<u>TGGGCTTCGGAATCGT</u> GCAACCCCAA CTCTATTGAGAGGTATTTTCA	
pABBR_Km_Km_Screen	TGATATTGCTGAAGAGCTTGGCG	Screening to confirm the cloning of the <i>goi</i> into pABBR_Km
qRT-PCR		
ESR		
degP_F_qPCR	GTAATCAGAGCACCTTCCGGTTTAG	Amplification of a portion of <i>degP</i>
degP_R_qPCR	TGACTCGTTCATACCTAGGCGTTAT	
baeR_F_qPCR	TGTTACAGTACCTTACGGCAAATC	Amplification of a portion of <i>baeR</i>
baeR_R_qPCR	GGTCAGGATGCTTACACGAACTTT	
rstA_F_qPCR	CGCCCACACTATCATCAACCAA	Amplification of a portion of <i>rstA</i>
rstA_R_qPCR	GCACCCATTTCCAGACCAAGTA	
dsbA_F_qPCR	GGGTAGTGTAATGGCAGCAGATTT	Amplification of a portion of <i>dsbA</i>
dsbA_R_qPCR	GGTACTTCCACTTTGCCTGGATTG	

Bolded nucleotides denote restriction site.

Bolded and underlined nucleotides denote the region of homology for the Gibson assembly.

REFERENCES

- Blattner, F.R. (1997) The complete genome sequence of *Escherichia coli* K-12. *Science* **277**: 1453-1462.
- Crépin, S., Ottosen, E.N., Peters, K., Smith, S.N., Himpsl, S.D., Vollmer, W., and Mobley, H.L.T. (2018) The lytic transglycosylase MltB connects membrane homeostasis and *in vivo* fitness of *Acinetobacter baumannii*. *Mol Microbiol* **109**(6):745-762
- Dozois, C.M., Dho-Moulin, M., Bree, A., Fairbrother, J.M., Desautels, C., and Curtiss, R. (2000) Relationship between the Tsh autotransporter and pathogenicity of avian *Escherichia coli* and localization and analysis of the *tsh* genetic region. *Infect Immun* **68**: 4145-4154.
- Gallagher, L.A., Ramage, E., Weiss, E.J., Radey, M., Hayden, H.S., Held, K.G., Huse, H.K., Zurawski, D.V., Brittnacher, M.J., and Manoil, C. (2015) Resources for genetic and genomic analysis of emerging pathogen *Acinetobacter baumannii*. *J Bacteriol* **197**: 2027-2035.
- Jacobs, A.C., Thompson, M.G., Black, C.C., Kessler, J.L., Clark, L.P., McQueary, *et al.* (2014) AB5075, a highly virulent isolate of *Acinetobacter baumannii*, as a Model Strain for the evaluation of pathogenesis and antimicrobial treatments. *MBio* **5**: e01076-01014.
- Simon, R., Priefer, U., and Pühler, A. (1983) A broad host range mobilization system for *in vivo* genetic engineering: Transposon mutagenesis in Gram negative bacteria. *Bio/Technology* **1**: 784-791.
- Tipton, K.A., Chin, C.-Y., Farokhyfar, M., Weiss, D.S., and Rather, P.N. (2018) Role of capsule in resistance to disinfectants, host antimicrobials, and desiccation in *Acinetobacter baumannii*. *Antimicrob Agents and Chemother* **62**(12):e01188-18.